

RESEARCH

Open Access



Dual energy CT-derived quantitative parameters and hematological characteristics predict pathological complete response in neoadjuvant chemoradiotherapy esophageal squamous cell carcinoma patients

Miaomiao Li^{1,2†}, Yongbin Cui^{3†}, Yuanyuan Yan⁴, Junfeng Zhao³, Xinjun Lin³, Qianyu Liu³, Shushan Dong⁵, Mingming Nie⁵, Yong Huang⁴, Baosheng Li^{3*†} and Yong Yin^{3*†}

Abstract

Purpose There is no gold standard method to predict pathological complete response (pCR) in esophageal squamous cell carcinoma (ESCC) patients before surgery after neoadjuvant chemoradiotherapy (nCRT). This study aims to investigate whether dual layer detector dual energy CT (DECT) quantitative parameters and clinical features could predict pCR for ESCC patients after nCRT.

Patients and methods This study retrospective recruited local advanced ESCC patients who underwent nCRT followed by surgical treatment from December 2019 to May 2023. According to pCR status (no visible cancer cells in primary cancer lesion and lymph nodes), patients were categorized into pCR group ($N=25$) and non-pCR group ($N=28$). DECT quantitative parameters were derived from conventional CT images, different monoenergetic (MonoE) images, virtual non-contrast (VNC) images, Z-effective (Z_{eff}) images, iodine concentration (IC) images and electron density (ED) images. Slope of spectral curve (λHU), normalized iodine concentration (NIC), arterial enhancement fraction (AEF) and extracellular volume (ECV) were calculated. Difference tests and spearman correlation were used to select quantitative parameters for DECT model building. Multivariate logistic analysis was used to build clinical model, DECT model and combined model.

Results A total of 53 patients with locally advanced ESCC were enrolled in this study who received nCRT combined with surgery and underwent DECT examination before treatment. After spearman correlation analysis and

[†]Miaomiao Li and Yongbin Cui contributed equally to this work and co-first author.

[†]Baosheng Li and Yong Yin contributed equally for this work.

*Correspondence:

Baosheng Li
baoshli1963@163.com

Yong Yin
yinyongsd@126.com

Full list of author information is available at the end of the article



multivariate logistic analysis, AEF and ECV showed significant roles between pCR and non-pCR groups. These two quantitative parameters were selected for DECT model. Multivariate logistic analysis revealed that LMR and RBC were also independent predictors in clinical model. The combined model showed the highest sensitivity, specificity, PPV and NPV compared to the clinical and DECT model. The AUC of the combined model is 0.893 (95%CI: 0.802–0.983). Delong's test revealed the combined model significantly different from clinical model ($Z = -2.741, P = 0.006$).

Conclusion Dual-layer DECT derived ECV fraction and AEF are valuable predictors for pCR in ESCC patients after nCRT. The model combined DECT quantitative parameters and clinical features might be used as a non-invasive tool for individualized treatment decision of those ESCC patients. This study validates the role of DECT in pCR assessment for ESCC and a large external cohort is warranted to ensure the robustness of the proposed DECT evaluation criteria.

Keywords Dual energy CT, Esophageal squamous cell carcinoma, Neoadjuvant chemoradiotherapy, Pathological complete response, Arterial enhancement fraction, Extracellular volume

Introduction

Esophageal cancer ranks as the seventh leading cause of cancer-related mortality and the eleventh most prevalent cancer globally [1]. In China, esophageal squamous cell carcinoma (ESCC) is the predominant histological subtype of esophageal cancer, and it is typically diagnosed at an advanced stage. The CROSS trial has demonstrated that neoadjuvant chemoradiotherapy (nCRT) combined surgery is effective method for locally advanced ESCC (LA-ESCC) compared to surgery alone, adding nCRT to surgery resulted in a 13% absolute survival benefit at 10 years for patients with LA-ESCC [2, 3]. Pathological complete response (pCR) is considered the optimal outcome of nCRT, as it can inform subsequent treatment strategies [4]. Patients who achieved pCR tend to have longer overall survival (OS), while those not may experience a shorter OS in the near future [5]. According to the CROSS trial, the pCR rate after nCRT is as high as one-third (49% for squamous cell carcinoma and 23% for adenocarcinoma).

Due to the complexity of surgery after nCRT and poor quality of life for LA-ESCC patients postoperatively, some studies have demonstrated that patients who achieved clinical complete response (cCR) following nCRT may not undergo surgery in favor of active surveillance [6, 7]. These studies have concluded that active monitoring offers comparable overall survival to surgical resection, while concurrently yielding significantly patients' quality of life [7]. However, pCR can only be confirmed by histopathological examination post-surgery. Current strategies rely on the determination of cCR typically through medical imaging combined with endoscopic biopsy or endoscopic ultrasonography after nCRT to assess the treatment response status. This method is invasive, cannot sample deep tissues, and does not accurately reflect the total tumor's treatment response status. Therefore, there is a critical need for a non-invasive and accurate method to predict pCR following nCRT in patients with LA-ESCC.

Contrast enhanced CT derived extracellular volume (ECV) were useful in distinguishing between pCR and non-pCR patients with rectal cancer patients who received nCRT [8]. However, conventional CT is constrained by suboptimal soft-tissue resolution and a paucity of quantitative parameters, significantly limiting its clinical utility in predicting pCR in ESCC patients [9]. Wang et al. [10] found that the functional parameters (such as total lesion glycolysis and metabolic tumor volume) of 18 fluorodeoxyglucose positron emission tomography/computed tomography (18 F-FDG PET/CT) have the excellent performance for predicting pCR after the neoadjuvant immunochemotherapy (nICT) in resectable ESCC. But, the scanning time of PET/CT is longer, and the cost of the examination is higher than CT examination. A meta-analysis shows that apparent diffusion coefficient (ADC) computed from diffusion weighted imaging (DWI) during nCRT might be the predictor to distinguish pCR and non-pCR groups in ESCC patients [11]. However, MR is not the routine examination strategy for ESCC patients. Therefore, developing a non-invasive and convenient method to accurately predict pCR status after nCRT for ESCC patients remains a major challenge.

Dual-layer dual energy CT (DECT) is a novel imaging modality, which provides various forms of quantitative images and parameters [12]. Currently, DECT is mainly used for judging the clinical staging, pathological grading, and prediction lymph node metastasis in ESCC [13–15]. However, there are fewer studies focused on prediction the pCR and prognosis for ESCC patients after nCRT by DECT [16, 17]. Liu et al. [16] reported that preoperative arterial phase normalized iodine concentration (A-NIC) derived from DECT served as a noninvasively predictor for early recurrence in patients with ESCC after radical esophagectomy. However, whether preoperative DECT can predict pCR in ESCC patients after nCRT is still unclear. Additionally, to achieve routine clinical application and improve the prediction accuracy, more meaningful biomarkers need to be incorporated into the pCR status prediction, such as neutrophil-to-lymphocyte

ratio (NLR), platelet-to-lymphocyte ratio (PLR), and lymphocyte-to-monocyte ratio (LMR) [18, 19]. Therefore, this study aims to combine quantitative parameters from DECT images, clinical characteristics, and hematological biomarkers to predict pCR in ESCC patients after nCRT, which could provide clinical application value for individual treatment.

Methods

Patient recruitment and treatment

This study was approved by the Institutional Review Board of Shandong Cancer Hospital according to the Helsinki Declaration, and the requirement to obtain informed consent from each participant was waived due to the retrospective study. The patients were retrospectively recruited from Shandong Cancer Hospital for the period December 2019 to May 2023. The inclusion criteria were as follows: (1) histologically confirmed locally advanced (T2-4aN+/-M0) ESCC (according to the eighth edition of the American Joint Committee on Cancer staging system) [20]; (2) all patients treatment with nCRT followed by esophagectomy and postoperative pathology; (3) the availability of pre-treatment DECT scans for parameters analysis; and (4) patients with complete documentation of baseline laboratory tests and clinical characteristics. The exclusion criteria were as follows: (1) patients received the treatment of immunotherapy during nCRT; (2) patients failed to complete therapy (radiation dose less than 40 Gy) or received concurrent chemoradiotherapy followed by esophagectomy (radiation dose more than 50 Gy); (3) patients experienced severe infection before nCRT that might influence peripheral blood cell counts; and (4) poor image quality, such as significant motion artifact. In our study, all patients were treated with the intensity-modulated radiation therapy (IMRT) technique at a prescription dose of 40, 41.4, or 45 Gy and were treated with cisplatin/Paclitaxel (TP) or cisplatin/fluorouracil (PF) chemotherapy during radiotherapy. Surgery was performed within 4 to 8 weeks after the completion of nCRT.

Clinical data collection and pathological assessment

Collection the clinical characteristics, such as age, gender, smoking history, alcohol history, tumor location, TNM stage, and peripheral hematological parameters prior to nCRT, including white blood cell count (WBC), neutrophil count (NEU), monocyte count (MO), absolute lymphocyte count (ALC), red blood cell (RBC), platelet count (PLT), hemoglobin (HGB), and albumin (ALB), prealbumin (PAB), hematocrit value (Hct). The NLR was defined as the NEU divided by the ALC. The LMR was calculated as the ALC divided by the MO. The PLR was calculated as PLT dividing by ALC. Since all patients had complete pre-treatment hematological testing, there

were no missing data in the hematological data for any of the recruited patients.

Surgical specimens were evaluated by two pathologists specializing in ESCC who were blinded to the clinical information and CT images. All patients underwent postoperative restaging according to the 8th AJCC staging system. The pCR status was defined as the absence of residual invasive disease and positive lymph nodes in all layers of the esophagus (ypT0N0), if else was defined as non-pCR [21].

CT image and quantitative parameters acquisition

Each patient underwent CT scanning prior to nCRT, performed by a dual-layer detector DECT scanner with 64 detector rows (iQon Spectral CT, Philips Healthcare, Best, the Netherlands). Patients were scanned in supine position and following scan presets were used: tube voltage 120 kVp, tube current modulation (Dose Right 3D-DOM, Philips Healthcare, Best, The Netherlands), pitch 0.671, rotation time 0.33 s, collimation 64×0.625 mm, matrix 512×512 . To monitor radiation dose, the volumetric CT dose index (CTDIvol) was recorded.

An automated injection system (Medrad Stellant CT injection system, Bayer Healthcare, Leverkusen, Germany) was used for intravenous, body weight adapted administration of iodinated contrast media (<55 kg: 1 mL/kg; 55–120 kg: 100 mL; > 120 kg: 120 mL; Accupaque 350 mg/mL, GE Healthcare) and a 30 mL saline flush. Flow rate was set to 3.0 mL/s. Bolus tracking technique was applied to start portal venous phase image acquisition during inspirational breath-hold 50s after reaching a threshold value of 150 Hounsfield units (HU) in the descending aorta. The arterial phase was scanned with a delay of 30 s, and the delayed phase was scanned with a delay of 60 s.

Two phases contrast enhanced DECT images were import into post-processing workstation (ISP version 12, Philips). The spectral based images (SBI) of two phases were separated into conventional CT images, monoenergetic (MonoE) images (40 keV, 70 keV and 100 keV), virtual non-contrast (VNC) images, Z-effective (Zeff) images, iodine density (IC) images and electron density (ED) images. The region of interest (ROI) was defined as the primary tumor, however, areas of necrosis as well as intraluminal measurements of air and food residues were avoided regarding the esophagus. In addition, the circular ROI with the a 10mm^2 area (ROI₂) was placed on abdominal aorta at the same level. The images of all patients were independently delineated by two experienced radiologists, each with over 10 years of specialized experience. In final, a senior radiologist with 15 years experiences rechecked the two different delineation and made the final delineation. All quantitative parameters

were derived from one SBI database with the same space structures. Thus, all quantitative parameters data from each SBI recorded by ROI, only IC were additionally recorded both on ROI and ROI₂. The average of the data recorded by the two radiologists was then used for subsequent analysis. In addition to directly obtaining DECT parameters, several formulas were used to calculate those parameters: Slope of spectral curve (λ HU) was generated using the formula: λ HU = $(CT_{40\text{keV}} - CT_{100\text{keV}}) / 60$, where $CT_{40\text{keV}}$ and $CT_{100\text{keV}}$ respectively represent the CT attenuation at 40 keV and 100 keV MonoE images. Normalized iodine ratios (NIC) were obtained by ROI/ROI₂ in IC images. Arterial enhancement fraction (AEF) was calculated by formula (1) and DECT-derived extracellular volume (ECV) was calculated by formula (2):

$$AEF = \frac{AIC}{DIC} \quad (1)$$

The AIC and DIC are the tumor's iodine concentration in arterial phase and delayed phase, respectively. The AEF-NIC is obtained through the NIC in the arterial phase dividing the NIC in the delayed phase.

$$ECV = (1 - Hct) \times \frac{DIC}{D_{ROI2}} \times 100\% \quad (2)$$

Hct stands for hematocrit, which represents the percentage of red blood cells in a person's blood. D_{ROI2} represents the arterial iodine concentration in delayed phase.

Statistical analysis

SPSS (Version 26.0, IBM), R (Version 4.2.1), and Python software (Version 3.7.0) were used for all analyses. The differences in continuous variables between the two sets were compared using the Mann-Whitney U test or independent-samples T test. The differences in categorical variables between the two sets were compared using the chi-square test or Fisher's exact test. Each P value was determined using a two-sided test. After that, Spearman correlation was conducted on DECT multi-parameters. DECT quantitative parameters that show significance in the difference test and have a correlation coefficient (R) less than 0.3 with other parameters are selected. Multivariate logistic analysis was used to build clinical model, DECT model, and combined model (all selected clinical characteristics and DECT quantitative parameters). The models' performance for predicting pCR was evaluated by sensitivity, specificity, positive predictive value (PPV), negative predictive value (NPV) and the area under the curve (AUC) of receiver operating characteristic (ROC) curve. Additionally, 1000 bootstrapping techniques were used to enhance the stability of the logistic regression model and the calibration curve were used to evaluate

the model's performance. The optimal cut-off value for the predictor was determined using the Youden index from the ROC curve analysis. To substantiate these findings, 95% confidence interval (CIs) for each metric were calculated. The CIs for each of the above metrics was calculated using the Bootstrap method of the pROC package in R software. Delong's test was used for comparing the AUC values. Differences with two-tailed $P < 0.05$ were considered statistically significant.

Results

Patient characteristics

This study included 53 patients with locally advanced ESCC who received nCRT combined with surgery and underwent spectral DECT scanning before treatment. The mean age of all patients was 61.28 ± 6.39 years, with 44 males (83.02%) and 9 females (16.98%). Middle esophageal tumors were present in 32 patients (60.4%) and lower esophageal tumors in 21 patients (39.6%). Four patients (7.55%) had T2 stage disease, 48 patients (90.57%) had T3 stage disease, and 1 patient (1.88%) had T4 stage disease. Among all patients, 25 (47.17%) achieved pCR after nCRT, while 28 patients (52.83%) achieved non-pCR. Table 1 displayed the baseline clinical characteristics of all enrolled patients in different groups.

Quantitative parameters and clinical characteristics selection

According to the Mann-Whitney U test of DECT quantitative parameters in patients, this study found that A-NIC ($P = 0.003$), AEF ($P = 0.005$), AEF-NIC ($P = 0.028$), ECV ($P = 0.024$), A-CT ($P = 0.001$), A-40 ($P = 0.003$), A-70 ($P = 0.001$), A-100 ($P = 0.003$), A-Zeff ($P = 0.007$), A-IC ($P = 0.002$), and A- λ HU ($P = 0.005$) were significantly different between pCR and non-pCR group in ESCC patients after surgery (Table 2). A correlation analysis was performed on quantitative parameters with $P < 0.05$ in the logistic regression analysis (Fig. 1). Considering the correlations between parameters, the study excluded those with strong correlations and included only AEF and ECV, along with all clinical features, in the multivariate logistic regression analysis. Multivariate logistic analysis revealed that LMR and RBC were independent predictors in clinical model for predicting pCR. In the combined model, the study found that ECV (Odds Ratio [OR]: 1.282, 95% confidence interval [CI]: 1.069–1.538, $P = 0.007$), AEF (OR: 1.062, 95% CI: 1.022–1.104, $P = 0.002$), RBC (OR: 1.426, 95% CI: 1.103–1.844, $P = 0.007$), and LMR (OR: 1.979, 95% CI: 1.176–3.330, $P = 0.010$) were independent predictors of pCR in ESCC patients after nCRT (Table S1, see the Additional file 1). The cut off values of combined model of AEF, ECV, RBC and LMR were 0.775, 26.718, 4.880, 4.195 respectively.

Table 1 Patients baseline clinical characteristics in different groups

Baseline clinical characteristics	Total (n = 53)	pCR group (n = 25)	Non-pCR group (n = 28)
Age, Mean ± SD	61.28 ± 6.39	61.92 ± 6.30	60.71 ± 6.53
Gender			
Female	9 (16.98%)	7 (28.00%)	2 (7.14%)
Male	44 (83.02%)	18 (72.00%)	26 (92.86%)
Smoking			
No	22 (41.51%)	11 (44.00%)	11 (39.29%)
Yes	31 (58.49%)	14 (56.00%)	17 (60.71%)
Location			
Middle	32 (60.38%)	15 (60.00%)	17 (60.71%)
Lower	21 (39.62%)	10 (40.00%)	11 (39.29%)
Alcohol			
No	21 (39.62%)	11 (44.00%)	10 (35.71%)
Yes	32 (60.38%)	14 (56.00%)	18 (64.29%)
T stage			
T2	4 (7.55%)	1 (4.00%)	3 (10.71%)
T3	48 (90.57%)	24 (96.00%)	24 (85.71%)
T4	1 (1.88%)	0	1 (3.58%)
N stage			
N0	19 (35.85%)	9 (36.00%)	10 (35.71%)
N1	25 (47.17%)	14 (56.00%)	11 (39.29%)
N2	9 (16.98%)	2 (8.00%)	7 (25.00%)
WBC, Mean ± SD (×10 ⁹ /L)	6.79 ± 2.17	6.67 ± 2.08	6.91 ± 2.28
ALC, Mean ± SD (×10 ⁹ /L)	1.81 ± 0.58	1.86 ± 0.53	1.76 ± 0.62
NEU, Mean ± SD (×10 ⁹ /L)	4.32 ± 1.78	4.16 ± 1.61	4.46 ± 1.95
MO, Mean ± SD (×10 ⁹ /L)	0.52 ± 0.24	0.48 ± 0.28	0.55 ± 0.19
RBC, Mean ± SD (×10 ¹² /L)	4.56 ± 0.41	4.64 ± 0.43	4.49 ± 0.38
HGB, Mean ± SD (×10 ⁹ /L)	142.28 ± 12.72	143.68 ± 12.31	141.04 ± 13.17
ALB, Mean ± SD (g/L)	43.99 ± 3.49	44.68 ± 3.46	43.36 ± 3.45
PAB, Mean ± SD (g/L)	0.24 ± 0.05	0.24 ± 0.06	0.24 ± 0.05
Hct, Mean ± SD	0.42 ± 0.04	0.43 ± 0.04	0.42 ± 0.04
PLT, Mean ± SD	244.96 ± 61.58	239.08 ± 59.67	250.21 ± 63.85
NLR, Mean ± SD	2.53 ± 1.13	2.33 ± 0.90	2.71 ± 1.29
PLR, Mean ± SD	145.67 ± 48.26	135.73 ± 40.88	154.55 ± 53.17
LMR, Mean ± SD	3.90 ± 1.77	4.50 ± 1.86	3.37 ± 1.52

The pCR status prediction

The AUC values of ROC curves were used to evaluate the pCR prediction ability for DECT parameters, clinical features, the combination of DECT parameters and clinical features. The ROC curves were shown in the Fig. 2A. The AUC values, PPV, NPV were shown in Table 3. The AUC values for DECT model which combined AEF and ECV was 0.786 (95% CI: 0.649–0.920), for clinical model was 0.694 (95%CI: 0.550–0.836), and for the combination of DECT parameters and clinical features, the AUC was

Table 2 Quantitative parameters in the pCR and non-pCR groups

Quantitative parameters	Total (n = 53)	pCR (n = 25)	Non- pCR (n = 28)	P
Arterial phase				
A-CT, M (Q ₁ , Q ₃)	62.50 (53.40, 75.80)	74.20 (61.40, 82.90)	57.25 (52.57, 65.23)	0.001
A-40, M (Q ₁ , Q ₃)	124.30 (103.60, 165.00)	162.60 (117.60, 179.30)	115.35 (98.30, 126.92)	0.003
A-70, M (Q ₁ , Q ₃)	66.10 (56.60, 78.70)	77.90 (62.40, 84.60)	59.40 (54.47, 67.90)	0.001
A-100, M (Q ₁ , Q ₃)	51.90 (44.90, 58.60)	56.90 (50.70, 62.00)	47.45 (42.05, 53.30)	0.003
A-λHU, M (Q ₁ , Q ₃)	1.29 (0.95, 1.80)	1.64 (1.05, 2.00)	1.12 (0.87, 1.34)	0.005
A-VNC, M (Q ₁ , Q ₃)	40.90 (30.15, 51.65)	42.16 (37.40, 47.20)	37.59 (32.65, 43.10)	0.086
A-Zeff, M (Q ₁ , Q ₃)	7.92 (7.75, 8.13)	8.06 (7.80, 8.20)	7.83 (7.74, 7.94)	0.007
A-IC, M (Q ₁ , Q ₃)	1.06 (0.81, 1.45)	1.38 (1.07, 1.61)	0.90 (0.75, 1.08)	0.002
A-NIC, Mean ± SD	0.13 ± 0.05	0.15 ± 0.05	0.11 ± 0.03	0.003
A-ED, Mean ± SD	104.03 ± 0.80	104.18 ± 0.76	103.90 ± 0.82	0.193
Delay phase				
D-CT, Mean ± SD	80.86 ± 15.22	83.98 ± 14.10	78.07 ± 15.88	0.160
D-40, Mean ± SD	181.54 ± 36.86	190.57 ± 31.45	173.48 ± 39.93	0.092
D-70, Mean ± SD	83.48 ± 15.16	86.82 ± 13.79	80.49 ± 15.93	0.130
D-100, Mean ± SD	58.95 ± 12.08	60.04 ± 13.56	57.97 ± 10.76	0.538
D-λHU, Mean ± SD	2.04 ± 0.51	2.18 ± 0.46	1.93 ± 0.52	0.072
D-VNC, Mean ± SD	41.64 ± 8.92	42.26 ± 9.94	41.09 ± 8.05	0.640
D-Zeff, Mean ± SD	8.20 ± 0.18	8.25 ± 0.15	8.16 ± 0.19	0.064
D-IC, Mean ± SD	1.63 ± 0.39	1.73 ± 0.34	1.55 ± 0.42	0.095
D-NIC, Mean ± SD	0.49 ± 0.09	0.51 ± 0.08	0.47 ± 0.09	0.069
D-ED, M (Q ₁ , Q ₃)	104.30 (103.70, 104.80)	104.30 (103.70, 105.20)	104.40 (103.70, 104.60)	0.636
Post-processing parameters				
AEF, Mean ± SD	0.71 ± 0.24	0.80 ± 0.26	0.62 ± 0.19	0.005
AEF-NIC, Mean ± SD	0.27 ± 0.09	0.29 ± 0.09	0.24 ± 0.07	0.028
ECV, Mean ± SD	28.55 ± 5.19	30.23 ± 4.33	27.04 ± 5.51	0.024

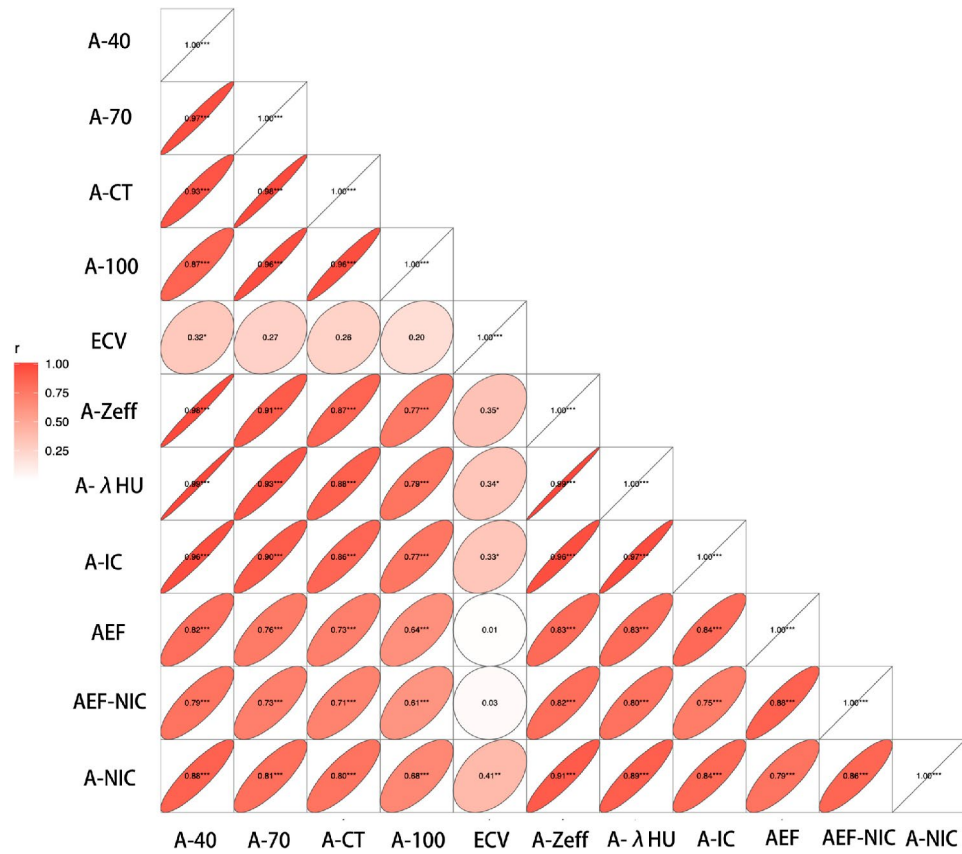


Fig. 1 The correlation of the DECT-derived quantitative parameters. Darker colors indicate higher correlations

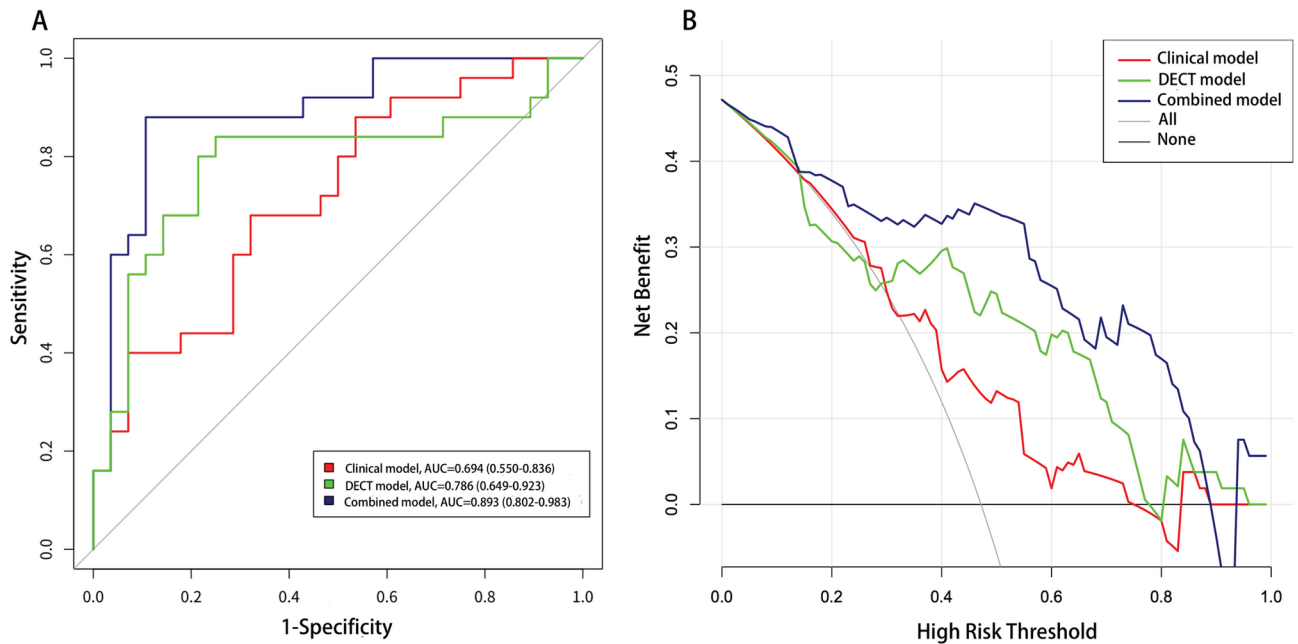


Fig. 2 The ROC curves (A) and DCA curves (B) of the three predictive model. DECT: dual energy CT; ROC: receiver operating characteristics curve; DCA: decision curve analysis

Table 3 The prediction ability for pCR in three model

	Sensi- tivity (95%CI)	Speci- ficity (95%CI)	PPV (95%CI)	NPV (95%CI)	AUC (95%CI)
Clinical model (sample size = 53)	0.520 (0.313– 0.722)	0.786 (0.590– 0.917)	0.684 (0.434– 0.872)	0.647 (0.465– 0.803)	0.694 (0.550– 0.836)
DECT model (sample size = 53)	0.680 (0.465– 0.851)	0.857 (0.673– 0.969)	0.819 (0.581– 0.946)	0.750 (0.566– 0.885)	0.786 (0.649– 0.920)
Combined model (sample size = 53)	0.880 (0.688– 0.975)	0.857 (0.673– 0.960)	0.846 (0.651– 0.956)	0.889 (0.708– 0.976)	0.893 (0.802– 0.983)

0.893 (95% CI: 0.802–0.983). The Delong’s test revealed that the combined model’s performance was significantly high than clinical model ($Z = -2.741, P = 0.006$). What’s more, the combined model demonstrated the best predictive performance among the three models, with a positive predictive value of 0.846 and a negative predictive value of 0.889.

Decision curve analysis (DCA) showed that the predictive models provided net benefits across different threshold probabilities, with the combination of DECT parameters and clinical features providing the best net benefit as shown in Fig. 2B. This suggests that the combination of DECT parameters and clinical features offers good potential clinical efficacy in predicting pCR. In Figure S1, the calibration curves were used to displayed the prediction ability of the three models. The ideal calibration curve indicated the actual treatment response results consistence with the predicted results. A curve closer to the ideal line demonstrated better predictive accuracy of the model. Fig. 3 displayed that the AEF and ECV were higher in pCR patients than non-pCR patients.

Discussion

This study demonstrated that DECT derived quantitative parameters and clinical characteristics were the significant predictors for pCR status in LA-ESCC patients after nCRT. Those parameters could be used to help clinicians selecting the most benefit ESCC patients from nCRT and making personal treatment strategy decision, such as organ preserve. To our knowledge, there are fewer studies exploring the prediction ability of DECT quantitative parameters for prediction pCR status in LA-ESCC patients after nCRT. We identify that AEF, ECV, RBC, and LMR are independent predictors of pCR and the prediction model integrating those predictors demonstrated superior prediction performance of pCR status, with the AUC values of 0.893.

AEF is an important parameter, which evaluates tumor tissue blood perfusion by analyzing the difference in iodine concentration between the arterial phase and other time points during contrast-enhanced CT [22]. Blood perfusion is closely related to tumor angiogenesis, proliferation, and invasion, difference of AEF in different time can be used to evaluate tumor response to treatment [23–25]. Mao et al. [23] found that AEF can be used to assess tumor response for hepatocellular carcinoma patients. Our study also found that increased AEF may be associated with the sensitivity of highly vascularized tumors to nCRT. The high iodine concentration indicates high vascular permeability, which allows chemotherapy drugs to penetrate more effectively into the tumor tissue, enhancing the therapeutic response. Previous studies have reported similar results, showing a significant correlation between AEF and the efficacy of nCRT in patients with rectal cancer [26]. In our investigation, the iodine concentration derived AEF as a biomarker reflects tumor

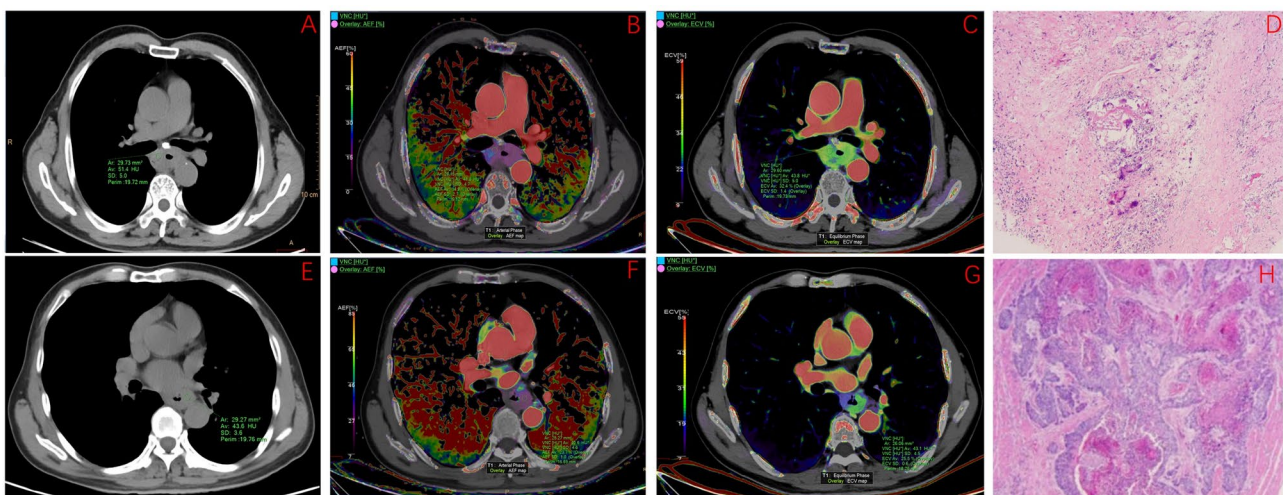


Fig. 3 Dual-energy CT quantitative parameters and pathological images of patients with pCR and non-pCR. A–D The CT images, AEF map, ECV map and pCR status images of a male patient. E–H The CT images, AEF map, ECV map and non-pCR status images of a male patient. The AEF and ECV values of the first patient were higher than the second patient

blood supply status, which has the clinical values in predicting the pCR status of ESCC patients after nCRT.

ECV reflects the proportion of extracellular matrix (ECM) within the tissue, which is an important parameter for assessing tissue fibrosis and changes in stromal components [27]. ECV has been widely applied as a non-invasive imaging parameter to assess treatment response in various cancers [8, 28, 29]. Studies have demonstrated that an increase in ECV generally indicates an accumulation of non-cellular components, which is closely related to tumor cell death induced by chemoradiotherapy [30]. Cai et al. [31] found that higher ECV values reflected significant tumor cell apoptosis and stromal remodeling in pancreatic cancer patients, which was associated with better survival rates following neoadjuvant chemotherapy. This finding aligned with our study. In esophageal cancer, chemoradiotherapy reduces tumor volume by inducing tumor cell apoptosis, a process accompanied by ECM accumulation and tissue fibrosis. Thus, an increase in ECV suggests greater ECM deposition within the tumor tissue, which may be associated with a favorable treatment response.

While both AEF and ECV individually demonstrated good predictive performance in forecasting pCR after nCRT in ESCC patients, our study revealed that combining these parameters significantly improved predictive accuracy (AUC = 0.786). This suggests that AEF and ECV have a complementary relationship, and their combination can reflect the biological characteristics of the tumor from different perspectives, providing more comprehensive predictive information. By jointly these two parameters according to the thresholds, clinicians can gain insights into both the hemodynamic properties and histological changes within the tumor, providing a more holistic basis for evaluating treatment response.

Our study also found that the LMR and RBC have the predictive values in determining pCR in ESCC patients following nCRT. Lymphocytes and monocytes are key components of the immune system, and LMR reflects the balance between host immune status and systemic inflammation [18]. A low LMR often indicates a reduction in lymphocytes or an increase in monocytes, which may suggest a weakened immune response and correlating with poor prognosis. Therefore, a low LMR may represent an immunosuppressive tumor microenvironment, potentially associated with resistance to chemoradiotherapy. RBC transports oxygen in blood vessel, which will alleviate tumor hypoxia in some extent. Our study indicates that an increased RBC count is associated with achieving pCR in ESCC patients following nCRT. This may reflect the role of RBC in improving local oxygen supply during treatment, thereby enhancing the effectiveness of radiotherapy. It is also noteworthy that an increased RBC count may reflect better physical

condition and bone marrow function, both of which are critical for tolerating chemoradiotherapy [32].

A recent study [16] found A-NIC can be used to non-invasively predict preoperative early recurrence (ER), but the AUC of A-NIC for predicting ER was only 0.72. Ge et al. [33] proved that DECT can be used to evaluate the efficacy of CRT for esophageal cancer, but they did not integrate clinical characteristic. Moore et al. [34] proposed that optimum tumor SUVmax decrease of FDG PET CT can be served as pathological tumor response prediction factor, but the AUC value was only 0.714. Xu et al. [35] found that combining ADC (Apparent Diffusion Coefficient) and TLG (total lesion glycolysis) can effectively predict pCR in ESCC patients after nCRT, with an AUC as high as 0.914, although MRI scan combined with PET-CT scan increased the physical and economic burden on patients. But, DECT was more feasible compared to PET or MR, and demonstrated superior predictive performance compared to conventional CT. In this study, a predictive model integrating DECT parameters and clinical characteristics was developed to predict pCR in ESCC patients undergoing nCRT followed by surgery. The model achieved an AUC of 0.893, outperforming both standalone DECT parameters and clinical features. It's potential to identify therapeutic-benefit patient subgroups and guide future treatment decision-making in the standard preoperative evaluation protocols.

However, our study still has some limitations. First, the sample size of patient cohort is relatively small. A larger cohort or external validation would further enhance the robustness and generalizability. Second, this is a retrospective study, suggesting a certain selection bias, which needs to be further verified in a large-scale prospective study. In the future, prospective validation in multicenter cohorts is critical to confirm the generalizability of our model. Third, despite histopathology is the gold standard for pCR evaluation, sampling errors, interobserver variability and the detectable of microscopic residual disease may also affect the accuracy of pCR assessment. Fourth, integrating our approach with complementary imaging modalities (e.g., dynamic contrast-enhanced MRI) or molecular biomarkers (e.g., circulating tumor DNA for longitudinal monitoring) could enable multimodal risk stratification. Finally, our quantitative parameters are derived solely from baseline DECT images; if DECT images following nCRT are available, those images might potentially provide more relevant information for organ preservation strategies.

Conclusion

DECT derived quantitative parameters, AEF and ECV can effectively predict pCR in ESCC patients after nCRT. Our study indicates that AEF, ECV, RBC, and LMR are all independent predictive factors, integrating the DECT

parameters and hematological parameters significantly improves the accuracy of predictions. The model combined DECT quantitative parameters and clinical features might provide additional information for individualized treatment decision of those ESCC patients. This study validates the role of DECT in pCR assessment for ESCC and a multi-center prospective validation cohort is warranted to further ensure the robustness of the proposed DECT evaluation criteria.

Abbreviations

DECT	Dual energy computer tomography
ESCC	Esophageal squamous cell carcinoma
pCR	Pathological complete response
nCRT	Neoadjuvant chemoradiotherapy
VNC	Virtual non-contrast
IC	Iodine concentration
ED	Electron density
NIC	Normalized iodine concentration
AEF	Arterial enhancement fraction
ECV	Extracellular volume
PPV	Positive predictive value
NPV	Negative predictive value
AUC	Area under curve
ROC	Receiver-operating characteristic
OS	Overall survival
cCR	Clinical complete response
MRI	Magnetic resonance imaging
PET/CT	Positron Emission Tomography/Computed Tomography
NLR	Neutrophil-to-lymphocyte ratio
PLR	Platelet-to-lymphocyte ratio
LMR	Lymphocyte-to-monocyte ratio
IMRT	Intensity-modulated radiation therapy
WBC	White blood cell count
NEU	Neutrophil count
MO	Monocyte count (MO), ALC: absolute lymphocyte count
PLT	Platelet count
HGB	Hemoglobin
ALB	Albumin
SBI	Spectral based images
ROI	Region of interest
DCA	Decision curve analysis
ECM	Extracellular matrix
RBC	Red blood cell

Supplementary Information

The online version contains supplementary material available at <https://doi.org/10.1186/s12876-025-03964-2>.

Supplementary Material 1

Acknowledgements

Thanks for Natural Science Foundation of China and all the clinician providing support during this study process.

Author contributions

All authors have evaluated the study and take responsibility for the integrity of the data analysis. Miaomiao Li and Yongbin Cui design the study and write the manuscript. Yuanyuan Yan, Junfeng Zhao, and Xinjun Lin acquired data and delineated the ROI. Qianyu Liu collected the data. Mingming Nie and Shushan Dong analyzed the data. Yong Huang evaluated the data. Baosheng Li and Yong Yin proposed the ideal and revised the study, Yong Yin also provided the funding.

Funding

This study is supported by the Natural Science Foundation of China (Grant No. 82072094 and 12275162).

Data availability

The datasets used and analyzed in this study are available from the corresponding author upon request.

Declarations

Ethics approval and consent to participate

This study was approved by the Ethics Committee of Cancer Hospital Affiliated to Shandong First Medical University, which waived the need for informed consent because of the retrospective nature of the study.

Consent for publication

Not applicable.

Competing interests

The authors declare no competing interests.

Author details

¹Shandong University Cancer Center, Shandong University, Jinan, Shandong, China

²Shandong Medical College, Jinan, Shandong, China

³Department of Radiation Oncology, Shandong Cancer Hospital and Institute, Shandong First Medical University, Shandong Academy of Medical Sciences, Jinan, Shandong, China

⁴Department of Radiology, Shandong Cancer Hospital and Institute, Shandong First Medical University, Shandong Academy of Medical Sciences, Jinan, Shandong, China

⁵Clinical Science, Philips Healthcare, Beijing, China

Received: 31 October 2024 / Accepted: 30 April 2025

Published online: 10 May 2025

References

- Bray F, Laversanne M. Global cancer statistics 2022: GLOBOCAN estimates of incidence and mortality worldwide for 36 cancers in 185 countries [J]. *CA Cancer J Clin*. 2024;74(3):229–63.
- Shapiro J, Van Lanschot J J B, Hulshof M, et al. Neoadjuvant chemoradiotherapy plus surgery versus surgery alone for oesophageal or junctional cancer (CROSS): long-term results of a randomised controlled trial [J]. *Lancet Oncol*. 2015;16(9):1090–8.
- Eyck B M, Van Lanschot J J B, Hulshof M, et al. Ten-Year outcome of neoadjuvant chemoradiotherapy plus surgery for esophageal cancer: the randomized controlled CROSS trial [J]. *J Clin Oncol*. 2021;39(18):1995–2004.
- Berger A C, Farma J, Scott W J, et al. Complete response to neoadjuvant chemoradiotherapy in esophageal carcinoma is associated with significantly improved survival [J]. *J Clin Oncol*. 2005;23(19):4330–7.
- Shen J, Kong M, Yang H, et al. Pathological complete response after neoadjuvant treatment determines survival in esophageal squamous cell carcinoma patients (NEOCRTEC5010) [J]. *Ann Transl Med*. 2021;9(20):1516.
- Tang H, Wang H, Fang Y, et al. Neoadjuvant chemoradiotherapy versus neoadjuvant chemotherapy followed by minimally invasive esophagectomy for locally advanced esophageal squamous cell carcinoma: a prospective multicenter randomized clinical trial [J]. *Ann Oncol*. 2023;34(2):163–72.
- Noordman B J, Wijnhoven B P L, Lagarde SM, et al. Neoadjuvant chemoradiotherapy plus surgery versus active surveillance for oesophageal cancer: a stepped-wedge cluster randomised trial [J]. *BMC Cancer*. 2018;18(1):142.
- Luo Y, Liu L, Liu D, et al. Extracellular volume fraction determined by equilibrium contrast-enhanced CT for the prediction of the pathological complete response to neoadjuvant chemoradiotherapy for locally advanced rectal cancer [J]. *Eur Radiol*. 2023;33(6):4042–51.
- Wongwaiyut K, Ruangsri S, Laohawiriyakamol S, et al. Pretreatment esophageal wall thickness associated with response to chemoradiotherapy in locally advanced esophageal Cancer [J]. *J Gastrointest Cancer*. 2020;51(3):947–51.
- Wang X, Yang W, Zhou Q, et al. The role of (18)F-FDG PET/CT in predicting the pathological response to neoadjuvant PD-1 Blockade in combination with

- chemotherapy for resectable esophageal squamous cell carcinoma [J]. *Eur J Nucl Med Mol Imaging*. 2022;49(12):4241–51.
11. Maffaioli L, Zilio M B, Klamt A L, et al. ADC as a predictor of pathologic response to neoadjuvant therapy in esophageal cancer: a systematic review and meta-analysis [J]. *Eur Radiol*. 2020;30(7):3934–42.
 12. Liu P, Lin L, Xu C, et al. Quantitative analysis of late iodine enhancement using dual-layer spectral detector computed tomography: comparison with magnetic resonance imaging [J]. *Quant Imaging Med Surg*. 2022;12(1):310–20.
 13. Yeo B, Shin K M, Park B, et al. Clinical feasibility of Dual-Layer CT with virtual monochromatic image for preoperative staging in patients with breast cancer: A comparison with breast MRI [J]. *Korean J Radiol*. 2024, 25(9).
 14. Wang Y, Tian W. Spectral CT - a new supplementary method for preoperative assessment of pathological grades of esophageal squamous cell carcinoma [J]. *BMC Med Imaging*. 2023;23(1):110.
 15. Gao L, Lu X, Wen Q, et al. Added value of spectral parameters for the assessment of lymph node metastasis of lung cancer with dual-layer spectral detector computed tomography [J]. *Quant Imaging Med Surg*. 2021;11(6):2622–33.
 16. Liu Y, Cheng F, Wang L et al. Quantitative parameters derived from dual-energy computed tomography for the preoperative prediction of early recurrence in patients with esophageal squamous cell carcinoma [J]. *Eur Radiol*, 2023.
 17. Gaber C E, Sarker J, Abdelaziz A I, et al. Pathologic complete response in patients with esophageal cancer receiving neoadjuvant chemotherapy or chemoradiation: A systematic review and meta-analysis [J]. *Cancer Med*. 2024;13(4):e7076.
 18. Goto W, Kashiwagi S, Asano Y, et al. Predictive value of lymphocyte-to-monocyte ratio in the preoperative setting for progression of patients with breast cancer [J]. *BMC Cancer*. 2018;18(1):1137.
 19. Hu X, Tian T, Sun Q, et al. Prognostic value of the neutrophil-to-lymphocyte ratio and platelet-to-lymphocyte ratio in laryngeal cancer: what should we expect from a meta-analysis? [J]. *Front Oncol*. 2022;12:945820.
 20. Rice T W, Ishwaran H, Ferguson M K, et al. Cancer of the esophagus and esophagogastric junction: an eighth edition staging primer [J]. *J Thorac Oncol*. 2017;12(1):36–42.
 21. Mandard AM, Dalibard F, Mandard JC, et al. Pathologic assessment of tumor regression after preoperative chemoradiotherapy of esophageal carcinoma. *Clinicopathol Correlat Cancer*. 1994;73(11):2680–6.
 22. Mahnken A H, Klotz E, Schreiber S, et al. Volumetric arterial enhancement fraction predicts tumor recurrence after hepatic radiofrequency ablation of liver metastases: initial results [J]. *Am J Roentgenol*. 2011;196(5):W573–9.
 23. Mao X, Guo Y, Wen F, et al. Applying arterial enhancement fraction (AEF) texture features to predict the tumor response in hepatocellular carcinoma (HCC) treated with transarterial chemoembolization (TACE) [J]. *Cancer Imaging*. 2021;21(1):49.
 24. Chai B, Xiang D, Wang W, et al. Arterial enhancement fraction in evaluating the therapeutic effect and survival for hepatocellular carcinoma patients treated with DEB-TACE [J]. *Cancer Imaging*. 2022, 22(1).
 25. Zhou Y, Xu Y K Gengd, et al. Added value of arterial enhancement fraction derived from dual-energy computed tomography for preoperative diagnosis of cervical lymph node metastasis in papillary thyroid cancer: initial results [J]. *Eur Radiol*. 2024;34(2):1292–301.
 26. Roeder F, Meldolesi E, Gerum S, Recent advances in (chemo-)radiation therapy for rectal cancer: a comprehensive review [J]. *Radiat Oncol*, 2020, 15(1).
 27. Sahai E, Atsaturov I. A framework for advancing our Understanding of cancer-associated fibroblasts [J]. *Nat Rev Cancer*. 2020;20(3):174–86.
 28. Fukukura Y, Kumagae Y, Higashi R, et al. Extracellular volume fraction determined by equilibrium contrast-enhanced multidetector computed tomography as a prognostic factor in unresectable pancreatic adenocarcinoma treated with chemotherapy [J]. *Eur Radiol*. 2018;29(1):353–61.
 29. Fukukura Y, Kumagae Y, Higashi R, et al. Extracellular volume fraction determined by equilibrium contrast-enhanced dual-energy CT as a prognostic factor in patients with stage IV pancreatic ductal adenocarcinoma [J]. *Eur Radiol*. 2020;30(3):1679–89.
 30. Zhao F, Pang G, Li X et al. Value of perfusion parameters histogram analysis of triphasic CT in differentiating intrahepatic mass forming cholangiocarcinoma from hepatocellular carcinoma [J]. *Sci Rep*, 2021, 11(1).
 31. Cai W, Zhu Y, Teng Z, et al. Extracellular volume-based scoring system for tracking tumor progression in pancreatic cancer patients receiving intraoperative radiotherapy [J]. *Insights Imaging*. 2024;15(1):116.
 32. Dicato M, Plawny L. Anemia in cancer [J]. *Ann Oncol*. 2010;21(Suppl 7):vii167–72.
 33. Ge X, Yu J, Wang Z, et al. Comparative study of dual energy CT iodine imaging and standardized concentrations before and after chemoradiotherapy for esophageal cancer [J]. *BMC Cancer*. 2018;18(1):1120.
 34. Moore JI, Subesinghe M, Santaolalla A, et al. Metabolic tumour and nodal response to neoadjuvant chemotherapy on FDG PET-CT as a predictor of pathological response and survival in patients with oesophageal adenocarcinoma [J]. *Eur Radiol*. 2023;33(5):3647–59.
 35. Xu X, Sun Z-Y, Wu H-W, et al. Diffusion-weighted MRI and 18F-FDG PET/CT in assessing the response to neoadjuvant chemoradiotherapy in locally advanced esophageal squamous cell carcinoma [J]. *Radiat Oncol*, 2021, 16(1).

Publisher's note

Springer Nature remains neutral with regard to jurisdictional claims in published maps and institutional affiliations.